NUCLEAR THEORY, Vol. 42 (2025)
eds. M. Gaidarov, N. Minkov, Heron Press, Sofia

Spectrum and Electromagnetic Properties of ^{24}Mg in the Geometric α-Cluster Model with $\mathcal{D}_{4h}$ Symmetry at Leading Order

G. Stellin[1,2], **K.-H. Speidel**[†3]

[1]ESNT and IRFU/DPhN, CEA Paris-Saclay, 91191 Gif-sur-Yvette, France
[2]IJCLab, CNRS-In2p3, Université Paris-Saclay, 91405 Orsay, France
[3]HISKP, Universität Bonn, Nußallee 14-16, 53115 Bonn, Germany

Abstract. The relevance of the point-symmetry group $\mathcal{D}_{4h}$ for the prediction of spectrum and electromagnetic properties of the ^{24}Mg nucleus is discussed in the framework of the geometric α-cluster model at leading order. The latter represents a macroscopic α-cluster framework wherein nuclear excitations are described in terms of rotations and vibrations of ^{4}He clusters about their equilibrium positions, at the vertices of a square bipyramid. The finite group associated with the latter regulates the composition of the rotational bands as well as the transitions between the energy levels, by means of additional selection rules, of molecular nature. A sample of reduced electric multipole transition probabilities of intraband nature is provided.

1 Introduction

The spectrum of the ^{24}Mg nucleus and its structural properties have been investigated far and wide, namely in relation with cluster configurations. In the literature, the intrinsic deformation of this open-shell isotope has been modeled by assuming an internal partition of the nucleons in two or more aggregates of nucleons, such as the 2α + ^{16}O [1], α + ^{20}Ne [1] and ^{12}C + ^{12}C [2–4] cluster configurations.

In more recent times, the antisymmetrized molecular dynamics (AMD) method has been applied to this nucleus, mostly with the purpose of analysing the intrinsic matter density distribution. So far, the latter has been studied for states lying in the two lowest $K^\pi = 0^+$ rotational bands and the lowest 2^+ band [5, 6], also in relation with isoscalar E0 [7] and E2 transitions [8]. In the latter work, the AMD approach has been combined with the generator coordinate method (GCM) with the purpose of processing a large number of basis wavefunctions [7]. The same method has been adopted for the structural analysis of the negative-parity states in the lowest $K^\pi = 0^-$ and 1^- bands in Ref. [9], whereas a more complete survey has been provided in Ref. [10], encompassing also the form factors.

In terms of *ab-initio* approaches, the ground state features have been analysed by nuclear lattice effective field theory (NLEFT) [11], adopting realistic nuclear forces drawn from chiral effective field theory (χEFT) at N^3LO. A NLEFT-based analysis of the structure of the excited states as in Ref. [12] is envisaged [13]. Additionally, isoscalar and isovector resonances have been investigated by means of the *ab-initio* projected generator coordinate method (PGCM) [14].

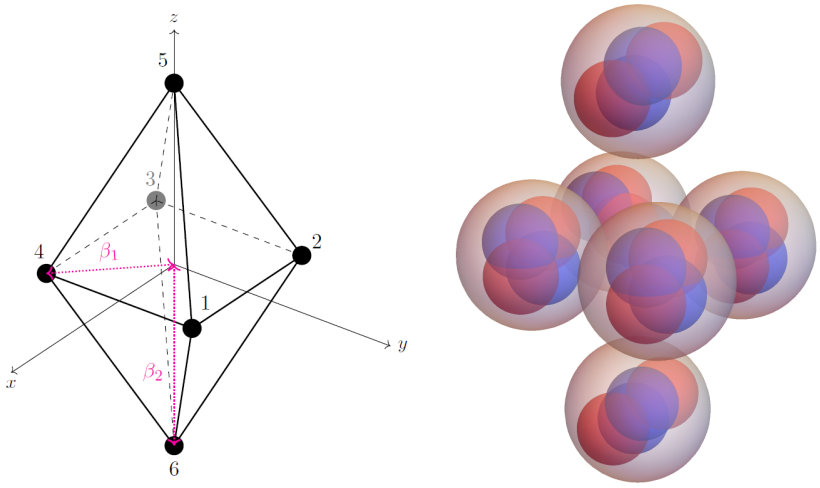

Figure 1. Equilibrium α-cluster configuration of ^{24}Mg in the intrinsic reference frame (left) with the underlying microscopic structure in terms for protons (red) and neutrons (blue) with realistic charge radii (right). The structure parameters (β_1, β_2), highlighted in red, are evaluated at $(2.380, 3.857)$ fm, corresponding to a prolate shape, consistently with the measured charge radius of the 0_1^+ state and the electric quadrupole moment of the 2_1^+ state. The charge distribution of the α-particles is assumed to be pointlike.

Macroscopic α-cluster models [15–17], *i.e.* phenomenological approaches employing the ^{4}He clusters as the sole degrees of freedom have been applied to light α-conjugate nuclei, mainly ^{12}C [18–22], ^{16}O [23–27] and ^{20}Ne [28]. Resting on the assumption that the oscillation period of the ^{4}He clusters is smaller or comparable with the diffusion time of a nucleon inside a cluster, nuclear excitations can be described in terms of rotating and vibrating of α-clusters around their molecular equilibrium configurations [16, 18]. The associated finite discrete symmetries are referred to as molecular or *exotic* nuclear symmetries [29, 30] and underlie also the more recent macroscopic α-cluster approaches, such as the *algebraic cluster model* (ACM) [31, 32] and the *quantum graph model* (QGM) [33–35]. The choice of the α-cluster ansatz is dictated by the number of bonds, n_b, between nearest-neighbour ^{4}He clusters; the spin and parity of the levels assigned in the literature to the *ground-state* (*g.s.*) rotational

band; the magnitude and the sign of the measured electric quadrupole moment of the nucleus in a state of the *g.s.* band.

Specifically, for ^{24}Mg, dihedral $\mathcal{D}_{4h}$ symmetry has quite firm roots in the literature [36–38]. The same point group appears in early applications [39] of the Bloch-Brink alpha-cluster model (BBACM) [40, 41]. The quite good agreement obtained with a $\mathcal{D}_{4h}$-symmetric elastic form factor [42] (cf. Sec. 3.1), the individuation of nine candidates for the lowest singly-excited rotational bands [43, 44] as well as the good accuracy measured reduced E0 and E2 transition probabilities recapitulated in Ref. [42] substantiate the adoption of the square-bipyramidal equilibrium configuration.

Finally, the flexibility of the formalism of the geometric α-cluster model (GαCM) allows for a systematic improvement in the prediction of nuclear observables, including the transition form factors, by considering the coupling between rotational and vibrational motion of the ^{4}He clusters.

2 Formalism

The theoretical framework is provided by the *geometric α-cluster model* (GαCM) [42, 43], describing the nucleus in terms of 6 α-particles rotating and vibrating about their equilibrium positions [45], located at the vertices of a square bipyramid (cf. Figure 1).

The most general Hamiltonian of a system of six harmonically vibrating and rotating clusters coincides with Watson's Hamiltonian [46], in which the two collective motions are completely coupled. Nonetheless, if the departures of the α-clusters, $\Delta\alpha_i$[1], from their equilibrium positions in the body-fixed reference frame, α_i^e, are small with respect to the size of the system, characterized by the parameters (β_1, β_2) in Figure 1, the rotation-vibration coupling contributions can be built up on top of the rigid-rotor Hamiltonian [42–44].

The vibrational degrees of freedom are encoded by the *normal coordinates* Q_i with $i = 1, \ldots 12$, whose significance can be understood graphically by expressing them in terms of the displacement coordinates $\Delta\alpha_i$ in the body-fixed frame. Under the constraint of normalization to $\sqrt{m}$ [43], the normal coordinates of the six non-degenerate modes take the form of Eqs. (13a)-(14f) in Ref. [43], with Q_1 and Q_2 in Eqs. (13a)-(13b) replaced by the linear combinations in Eqs. (3) and (4) of Ref. [44]. The choice is legitimate, since the original modes in Eqs. (13a)-(13b) in Ref. [43] Q_1 and Q_2 transform according to the same irreducible representation of the symmetry group associated with the equilibrium configuration of the α-particles, $\mathcal{D}_{4h}$. The latter consists of 16 elements, corresponding to proper and improper rotations (cf. Ref. [43] for the character table). For the 10 irreducible representations "irreps" of $\mathcal{D}_{4h}$, Mulliken's notation [47] is adopted.

[1]The notation of Refs. [43, 45, 48] is adopted: $\alpha, \beta, \gamma \ldots = x, y, z$ ($A, B, C, \ldots = \xi, \eta, \zeta$) denote the Cartesian components of tensors defined in the body-fixed or *intrinsic* (laboratory) frame.

In particular, the coordinate Q_1' represents an asymmetric *stretching* mode and transforms according to the A_{1g} representation of $\mathcal{D}_{4h}$, whereas Q_2' is a symmetric *stretching* or "breathing" mode, with the same transformation properties under the equilibrium symmetry group (cf. Fig. 2 of Ref. [44]). Conversely, the Q_3 mode denotes a symmetric *wagging* mode (irrep A_{2u}), the Q_4 an asymmetric *stretching* mode (irrep B_{1g}), the Q_5 a symmetric *scissoring* mode (irrep B_{2g}) and the Q_6 a symmetric *twisting* mode [42] (irrep B_{2u}). Next, the coordinates (Q_7, Q_8) represent an asymmetric *twisting* mode (irrep E_g), the (Q_9, Q_{10}) an asymmetric *scissoring* mode (irrep E_u) and the (Q_{11}, Q_{12}) an asymmetric *rocking* mode [42] (irrep E_u) [43].

From the expansion of the inverse effective inertia tensor in Watson's Hamiltonian [46], it is possible to construct a tower of systematically-improved Hamiltonians, H_{LO}, H_{NLO}, $H_{N^2LO}\ldots$ [42] corresponding to higher-order rotation-vibration correlations built on top of the uncorrelated "reference" Hamiltonian, H_{LO}. A survey of systematic approximation schemes for Watson's Hamiltonian in molecular physics is provided in Ref. [49].

The various interaction terms coupling rotations with vibrations might be treated in perturbation theory, built on top of the reference LO Hamiltonian. In general, the corrections do not conserve $\mathcal{D}_{4h}$ symmetry and induce triaxiality, although to different extent, depending on the truncation scheme. In particular, the LO Hamiltonian coincides with the well-known *rigid-rotor* limit in Eq. (7) of Ref. [44], where $(\omega_1, \omega_2, \omega_3, \omega_4, \omega_5, \omega_6, \omega_7, \omega_7, \omega_8, \omega_8, \omega_9, \omega_9)$ are the *frequencies* associated with the normal modes with coordinates $Q_1,\ Q_2,\ \ldots\ Q_{12}$ respectively and

$$I_{xx}^{\text{stat}} = I_{yy}^{\text{stat}} = 2m(\beta_1^2 + \beta_2^2)\,, \tag{1a}$$

$$I_{zz}^{\text{stat}} = 4m\beta_1^2\,, \tag{1b}$$

are the only non-vanishing components of the static inertia tensor, as the axes of the body-fixed frame are parallel to the principal axes of inertia of the square bipyramid and $m \approx 3727.4$ MeV is the α-particle mass. The invariances of H_{LO} are larger than the ones of Watson's Hamiltonian [46], since rotations and vibrations are decoupled and the system behaves as a symmetric top.

Since H_{LO} commutes with the components of the *rotational* angular momentum operator in the laboratory frame, J_ξ, J_η and J_ζ, as well as with J_z (cf. their expressions in terms of the Euler angles (χ, θ, φ) in the active picture [50] in Ref. [43]), the eigenvalues of Eq. (7) of Ref. [44] admit an expression in closed form,

$$E_{LO}(J, K, [\mathfrak{n}]) = \frac{\hbar^2}{2I_{xx}^{\text{stat}}}[J(J+1) - K^2] + \frac{\hbar^2 K^2}{2I_{zz}^{\text{stat}}} - \frac{\hbar^2}{8}\sum_\alpha {I_{\alpha\alpha}^{\text{stat}}}^{-1} + \sum_{i=1}^{6}\hbar\omega_i(\mathfrak{n}_i + \frac{1}{2}) + \sum_{i=7}^{9}\hbar\omega_i(\mathfrak{n}_i + 1)\,, \tag{2}$$

where $\hbar K$ ($\hbar M$) is the angular momentum projection along the intrinsic (laboratory-fixed) z-axis and $\hbar^2 J(J+1)$ is the eigenvalue of the quadratic Casimir operator of $\mathfrak{so}(3)$, J^2. In Eq. (2), the number of vibrational quanta or "phonons" for the normal modes $\mathfrak{n}_i$ are vectorized as $[\mathfrak{n}]$, where $i = 1, 2 \ldots 9$, because the modes $i = 7, 8$ and 9 are two-dimensional.

Since rotations and vibrations are decoupled, the eigenstates of H_{LO} can be factorized into a vibrational part, ψ_V, and a rotational part, ψ_R. Nonetheless, due to the presence of a combination of an axial symmetry and a point-group symmetry, $\mathcal{D}_{4h}$, the factorization of the eigenstates of H_{LO} into rotational and vibrational states (cf. Secs. 4-2c and 4-2d of Ref. [51]) is no longer valid.

By denoting the vibrational quanta with the frequencies ω_i, *i.e.* $\nu_i = \mathfrak{n}_i$ with $i = 1, 2, \ldots 6$ for the non-degenerate modes and $\nu_7 + \nu_8 = \mathfrak{n}_7$, $\nu_9 + \nu_{10} = \mathfrak{n}_8$ and $\nu_{11} + \nu_{12} = \mathfrak{n}_9$ for the doubly-degenerate ones as in Ref. [43], the restrictions imposed on the LO eigenfunctions by the $\mathcal{D}_{4h}$ group result into

$$\Psi^{\mathcal{D}_{4h}}_{RV}(\mathbf{Q}, \mathbf{\Omega}) = \sqrt{\frac{(2J+1)}{32\pi^2 \Delta(\mathfrak{n}, K)}} \Big\{ \left[\psi_V + (-i)^K \bar{\psi}_V\right] D^{J*}_{-KM}(\chi, \theta, \varphi) + (-1)^{J+K+\nu_3} \left[\psi_V + i^K \bar{\psi}_V\right] D^{J*}_{KM}(\chi, \theta, \varphi) \Big\}, \quad (3)$$

where $D^{J*}_{KM}(\chi, \theta, \varphi)$ are Wigner D-matrices in the active picture [50], $\mathbf{Q}$ denotes the normal coordinates in vector form, $\mathbf{\Omega}$ the Euler angles and $\Delta(\mathfrak{n}, K) \equiv (\delta_{K0} + 1)(1 + \delta_{\nu_7\nu_8}\delta_{\nu_9\nu_{10}}\delta_{\nu_{11}\nu_{12}})$ a prefactor. In Eq. (3), ψ_V represents the vibrational part of the the LO eigenfunction, defined in Eqs. (12)-(13) of Ref. [44], whose transformation properties under $\mathcal{D}_{4h}$ are recapitulated in Tabs. 2-3 in Ref. [43]. For the Wigner D-matrices, direct inspection of their transformation properties under the equilibrium symmetry group delivers the results in Tab. 4 of Ref. [43]. Additionally, the two terms enclosed by the square brackets on the r.h.s. of Eq. (3) are mapped one another by time reversal, $\mathscr{T}$, and the "partner" of ψ_V, $\bar{\psi}_V$, has been introduced as in Eq. (16) of Ref. [44]. Moreover, if $\nu_i = \nu_{i+1}$ in all the doubly-degenerate modes, the states in Eq. (3) reacquire the factorized form between the vibrational and the rotational part, even when $K \neq 0$.

At LO, the eigefunctions of the Hamiltonian have well-defined transformation properties under the operations of $\mathcal{D}_{4h}$ as well as parity, $\mathscr{P}$, and time-reversal, $\mathscr{T}$ [43, 44]. Consequently, the $\Psi^{\mathcal{D}_{4h}}_{RV}$'s transform as the irreducible representations A_{1g} and the A_{1u} [43] of $\mathcal{D}_{4h}$, associated with even and odd parity states respectively (cf. Tab. 5 of Ref. [43] and Tab. I of Ref. [52]).

Besides the energy eigenstates, for the validation of the $\mathcal{D}_{4h}$-symmetric structural ansatz, it is important to focus on the observables related to γ-transitions and electron scattering on the ^{24}Mg nucleus. In the GαCM framework, the squared transition form factors between two rotational-vibrational eigenstates with fixed J, K, M and $[\mathfrak{n}]$ are defined as

$$|F(\mathbf{q}, J_i^{\pi_i}, K_i, [\mathfrak{n}]_i \to J_f^{\pi_f}, K_f, [\mathfrak{n}]_f)|^2 \equiv$$
$$\frac{1}{2J_i+1} \sum_{M_i=-J_i}^{J_i} \sum_{M_f=-J_f}^{J_f} |\langle J_f, M_f, |K_f|, [\mathfrak{n}]_f | F(\mathbf{q}) | J_i, M_i, |K_i|, [\mathfrak{n}]_i \rangle|^2 \,, \quad (4)$$

where $F(\mathbf{q})$ is the form-factor operator in the laboratory frame. In the intrinsic frame, this operator takes the form in Eq. (19) of Ref. [44] and depends on the α-particles' positions in the intrinsic frame, $\mathbf{r}_i \equiv (x_i, y_i, z_i)$, hence on the normal coordinates. Approximations to the exact expression of the squared form-factors can be obtained by evaluating the operator in Eq. (19) of Ref. [44] at the equilibrium α-particles' positions (static limit), $\mathbf{r}_i^e \equiv (x_i^e, y_i^e, z_i^e)$ as in Refs. [28, 52]. Specifically, for a $\mathcal{D}_{4h}$-symmetric configuration and transitions between the ground state and states with zero vibrational quanta, one obtains

$$F_{\text{stat}}(\mathbf{q}, 0^+, 0, [\mathbf{0}] \to J_f^{\pi_f}, K_f, [\mathfrak{n}]_f) \equiv$$
$$\frac{\sqrt{4\pi}}{6} j_{J_f}(q\beta_1) \mathrm{f}(q) \sum_{\ell=0}^{3} Y_{J_f, |K_f|}\Big(\frac{\pi}{2}, (2\ell+1)\frac{\pi}{4}\Big)$$
$$+ \frac{\sqrt{4\pi}}{3} j_{J_f}(q\beta_2) \mathrm{f}(q) \sqrt{\frac{2J_f+1}{4\pi}} \Big(\frac{1+(-1)^{J_f}}{2}\Big) \delta_{K_f 0} \,, \quad (5)$$

where $Y_\lambda^{\nu *}$ is a spherical harmonic, j_{J_f} is a spherical Bessel function and $\mathrm{f}(q) = 1$ for a pointlike charge distribution for the ^{4}He clusters and $|K_f| = 0, 4, 8 \ldots$. For a spherical Gaussian profile of charge distribution $\mathrm{f}(q) = \exp(-q^2/4\alpha_1)$ with $\alpha_1 = 0.53$ fm^{-2}, as in Ref. [28].

Next, one considers the γ-transitions between the various energy states lying in the rotational bands of ^{24}Mg. Although of different nature, electric monopole transitions are often included in the set. The reduced electric ($R = E$) or magnetic ($R = M$) multipole transition probability between the initial state $(\Psi_{RV}^{\mathcal{D}_{4h}})_i$ characterized by the parity π_i, the quantum numbers J_i, M_i, K_i and $[\mathfrak{n}]_i$ phonons, and the final state $(\Psi_{RV}^{\mathcal{D}_{4h}})_f$ with parity π_f and the quantum numbers J_f, M_f, K_f and $[\mathfrak{n}]_f$, is provided by

$$B(R\lambda, J_i^{\pi_i}, |K_i|, [\mathfrak{n}]_i \to J_f^{\pi_f}, |K_f|, [\mathfrak{n}]_f) = \frac{1}{2J_i+1} \sum_{Mi=-J_i}^{J_i} \sum_{Mf=-J_f}^{J_f}$$
$$\times \sum_{\mu=-\lambda}^{\lambda} |\langle J_f, M_f, |K_f|, [\mathfrak{n}]_f | \Omega_{\lambda\mu}(R) | J_i, M_i, |K_i|, [\mathfrak{n}]_i \rangle|^2 \,, \quad (6)$$

where $\Omega_{\lambda\mu}(R)$ is the transition operator in the laboratory frame, connected with the intrinsic counterpart, $\omega_{\lambda\mu}(R)$, through Eq. (22) of Ref. [44]. Finally, one defines the EM moments which characterize a given rotational-vibrational state of parity π, angular momentum J, projection $|K|$ on the intrinsic frame and $[\mathfrak{n}]$

vibrational quanta. Setting the angular-momentum projection to the maximum value on the laboratory frame, $M = J$, the magnetic dipole moment is given by Eq. (24) of Ref. [44], whereas the electric quadrupole moment yields Eq. (25) of Ref. [44]. Higher-order EM moments are treated only in Ref. [42].

3 Low-Energy Spectrum and γ-Transitions

In the present model, the observed J^π energy states are grouped into rotational bands, characterized by $|K|^\pi$, the number of vibrational quanta $[\mathfrak{n}]$ in the vibrational part of the assigned $\Psi_{RV}^{\mathcal{D}_{4h}}$ states and (a direct sum of) irreducible representations of $\mathcal{D}_{4h}$ associated with the corresponding excited normal mode(s). As for ^{12}C [18,31,53], ^{16}O [24,27] and ^{20}Ne [28], not all the observed low-energy spectrum is susceptible to a description in terms of ^{4}He clusters.

Representatives for all the singly-excited vibrational modes have been detected [42,43], and the composition of the lowest-$|K|$ bands is mostly coherent with the literature [2,8,54–56]. The classification of states into bands with definite $|K|$ value remains valid in good approximation also for models which consider the ^{24}Mg nucleus as triaxial [1], such as the α-particle models with a $\mathcal{D}_{2h}$-symmetric equilibrium structure [41,52].

Concerning the γ-transition strengths, the available results of the $\mathcal{D}_{4h}$-symmetric GαCM at LO deliver results which are capable of capturing the established trends in the observed rotational bands $|K|^\pi$ [44]. Nonetheless, the measured EM multipole transition probabilities represent only a small portion of the allowed transitions between the states classified into the $|K|^\pi = 0^+$ unexcited band and the nine singly-excited rotational bands with lowest $|K|$ value. The presence of $\mathcal{D}_{4h}$ symmetry imposes additional selection rules, *i.e.* constraints on the γ-transition modes based on the vanishing integral rule [48], and are discussed extensively in Ref. [43]. For the sake of brevity, only the results involving the ground-state band are reported, whereas vibrational excitations as the associated transitions at LO are covered in Refs. [42,44], hence are left aside this proceedings.

3.1 Unexcited bands

For the bands corresponding to zero vibrational excitation, $\mathfrak{n} = 0$, the GαCM predicts rotational bands with $|K| = 0, 4, 8\ldots$, all with positive parity [43,52]. The one with $|K|^\pi = 0^+$ coincides with the ground-state band and is made of states with positive total angular momentum. In the observed spectrum, its composition is well-established [57] (cf. Table 1).

The measured nuclear properties include the charge radius of the 0_1^+ state, equal to $\sqrt{\langle r^2\rangle_{g.s.}} = 3.0570(16)$ fm [58], the electic quadrupole moment of the 2_1^+ state, equal to $Q = -29.0(30)\ e\ \mathrm{fm}^2$ [59] or $-16.6(6)\ e\ \mathrm{fm}^2$ [60] and the

[1] T. Otsuka, *A novel overall view of nuclear shapes, rotations and vibrations*, European Nuclear Physics Conference, Caen (2025)

Table 1. The ground-state $|K|^\pi = 0^+$ band of ^{24}Mg, corresponding to zero quanta of vibrational excitation (A_{1g} irrep). The calculated energy states refer to the parameter sets $(\beta_1, \beta_2) \approx (2.247, 3.566)$ and $(2.380, 3.857)$ fm. The composition reflects the one in the NNDC/ENSDF database, except for the inclusion of the 8^+ line at 11.860 MeV

A_{1g} (g.s.) BAND		Exper. [MeV]	GαCM LO (β_1, β_2) [e fm^2]	
J^π	Refs.	Ref. [57]	$(2.25, 3.57)$ fm	$(2.38, 3.86)$ fm
0^+	[2,7,8,10,55]	0.0(0)	0.0	0.0
2^+	[2,7,8,10,55]	1.368667(5)	0.882	0.762
4^+	[2,7,8,10,55]	4.122853(12)	2.940	2.543
6^+	[2,7,8,10,55]	8.1132(10)	6.174	5.340
8^+	New assignment	11.860(2)	10.584	9.155

magnetic dipole moments of the 2_1^+ and 4_1^+ states, equal to $\mu = -1.08(3)\mu_N$ [59] and $+1.7(12)\mu_N$ [59] respectively. Consequently, the nucleus has a marked prolate deformation and α-cluster character [61].

Fitting the structure paramaters of the nucleus, β_1 and β_2 on the experimental charge radius and the E2 moment in Ref. [60], one obtains the set $(\beta_1, \beta_2) \approx (2.247, 3.566)$ fm, whereas, with the quadrupole moment in Ref. [59] one obtains $(\beta_1, \beta_2) \approx (1.812, 4.031)$ fm. Since the charge radius of the α-particle is equal to $1.6755(28)$ fm [58], the measurement in Ref. [60] is more compatible with the chosen square bipyramidal α-structure, as it minimizes the overlap between the planar ^{4}He clusters as for ^{20}Ne [28]. Apart these sets of structure parameters, one might consider to fix β_1 on the minimum distance to avoid overlap between the planar α-particles and adjust β_2 on the average between the value wihch delivers the best fit to the ^{24}Mg charge radius and the E2 moment in Ref. [59], obtaining $(\beta_1, \beta_2) \approx (2.380, 3.857)$ fm.

Recent investigations on the ground state based on the AMD approach combined with the GCM [8,9] suggest that the 0_1^+ state of the nucleus has a Bohr-Mottelson quadrupole deformation [51] parameter $\beta = 0.49$, together with a mild triaxiality, $\gamma = 13°$. In the LO GαCM, one obtains $\beta \approx 0.57$ (1.12) from the parameter set based on the electric quadrupole moment in Ref. [60] ([59]), whereas from the set $(\beta_1, \beta_2) \approx (2.380, 3.857)$ fm the value $\beta \approx 0.60$ is found. Consequently, the set $(\beta_1, \beta_2) \approx (1.812, 4.031)$ fm can be left aside, for reasons of compatibility, also with the early calculations in the framework of Nilsson's microscopic rotational model.

Regarding the moments of inertia, the deviation between the *rigid-rotor* estimate and the counterpart obtained from the interpolation on the experimental energies of the states lying in the $|K|^\pi = 0^+$ band are, in general, larger than the statistical errors. Similar discrepancies are highlighted in Ref. [28], where the same approach has been applied to LO for ^{20}Ne. Specifically, for the ground-state band of ^{24}Mg, one has a nucleon-mass-specific moment of inertia [28] with respect to the x (z) axis of 125.5(78) fm^2 (24.0(131) fm^2). For the

Table 2. Quadrupole moments of the states belonging to the lowest $|K|^\pi = 0^+$ band of ^{24}Mg, corresponding to zero vibrational quanta (A_{1g} irrep). The calculated E2 moments states refer to the parameter sets $(\beta_1, \beta_2) \approx (2.247, 3.566)$ and $(2.380, 3.857)$ fm

A_{1g} (g.s.) BAND	EXPER. [e fm^2] Ref. [60]	Ref. [59]	GαCM LO (β_1, β_2) [e fm^2] $(2.25, 3.57)$ fm	$(2.38, 3.86)$ fm
$Q[2^+]$	$-16.6(6)$	$-29.0(30)$	-16.60	-20.15
$Q[4^+]$	n.a.	n.a.	-21.13	-25.64
$Q[6^+]$	n.a.	n.a.	-23.24	-28.21
$Q[8^+]$	n.a.	n.a.	-24.46	-29.69

same band, with the structure parameters (β_1, β_2) adjusted to $(2.247, 3.566)$ and $(1.812, 4.031)$ fm, one obtains 142.1 fm^2 (80.8 fm^2) and 156.3 fm^2 (52.5 fm^2) respectively. For the fit of the moment of inertia along the z axis, the sequence headed by the 4^+ state at 8.43929(5) MeV and followed by a $(6)^{(+)}$ at 12.7333(6) MeV, a 8^+ state at 17.90(1) MeV and a $(10)^{(+)}$ state at 23.26(1) MeV has been exploited as $|K|^\pi = 4^+$ sideband [37].

At LO, the electric quadrupole moment has been calculated for all the detected states of the lowest $|K|^\pi = 0^+$ band (cf. Table 2). Despite the fact that β_2

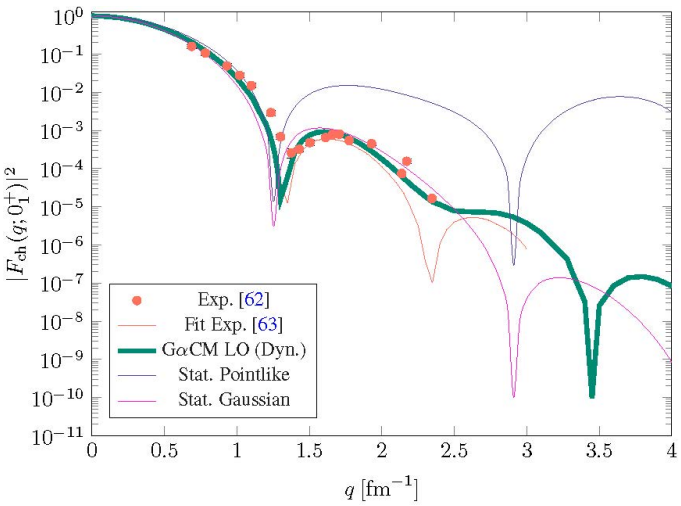

Figure 2. Squared charge form factor of the ground state 0^+ of the ^{24}Mg nucleus. The measured dataset in Ref. [62] is superimposed by its fit in Ref. [63] (thin orange curve). The theoretical results in the static limit in Eq. (5) for pointlike (thin purple curve) and spherical Gaussian (thin magenta curve) α-clusters are superimposed, together with the GαCM counterpart at LO with the parameter set $(\beta_1, \beta_2) \approx (2.247, 3.566)$ fm (thick light blue curve).

in the parameter set $(\beta_1, \beta_2) \approx (2.380, 3.857)$ fm is obtained from an average between the β_2 value wihch gives the best fit to the ^{24}Mg charge radius and the E2 moment in Ref. [59], the E2 moment estimate for the 2_1^+ state is in better agreement with the measurement in Ref. [60].

Furthermore, the elastic form factor for the 0_1^+ state, $F_{\rm ch}(q; 0_1^+)$, has been analyzed, by considering the limit $J_i = J_f = 0$ in the expression in Eq. (4), which represents the *dynamic* limit of the one in Eq. (5). Taking the squared modulus of the latter, one obtains the curves in Figure 2, in which the experimental counterpart is taken from Ref. [62]. The fit of the displayed experimental dataset performed in Ref. [63], highlights a very good agreement of the GαCM LO prediction with the observed minimum at $q \approx 1.35$ fm^{-1}, with deviations of 0.05 fm^{-1}. A similar accuracy for the first minimum is reached by the Gaussian static approximation in Eq. (5), but for the second minimum the effects of the dynamics, *i.e.* the normal coordinates, are evident. Overall, the two curves deliver a good order-of-magnitude estimate of $|F_{\rm ch}(q; 0_1^+)|^2$. In constrast, the pointlike approximation for the α-particles is incapable of capturing the correct order of magnitude of the squared elastic form factor for $q \gtrsim 1.2$ fm. Concerning the transition form factors, the analysis is carried out in Ref. [42].

Next, the intraband γ-transitions have been calculated. For processes of elecric quadrupole type, the application of the identity in Eq. (6) delivers the results in Table 3 for the parameter sets $(\beta_1, \beta_2) \approx (2.247, 3.566)$ and $(2.380, 3.857)$ fm. Higher-order electric even multipolarities have not been measured yet, as well as M1 or M3 transitions. For the parameter set $(\beta_1, \beta_2) \approx (2.380, 3.857)$ fm, the displayed E2 reduced transition probabilities are in excellent agreement with the experimental counterparts. The other structure parameter set ensures at least order-of-magnitude agreement with the measured transition strengths, with an underestimation of 20-25% on average. In the AMD application in Ref. [8], the reduced E2 transition probabilities of the lowest $|K| = 0$ band are reproduced with an accuracy ranging from 4 to 26%.

Table 3. Reduced E2 transition probabilities among the states of the ground-state band of ^{24}Mg, corresponding to zero quanta of vibrational excitation. In the limit $\beta_1 = \beta_2$, the GαCM predictions at LO vanish

INTRABAND A_{1g} (g.s.)	EXPERIMENTAL [57] [W.u.]	EXPERIMENTAL [57] [e^2 fm^4]	GαCM LO (β_1, β_2) [e^2 fm^4] $(2.25, 3.57)$ fm	$(2.38, 3.86)$ fm
$\mathrm{B}[E2; 0^+ \to 2^+]$	105.5^{+240}_{-230}	433.24^{+987}_{-946}	327.14	484.13
$\mathrm{B}[E2; 2^+ \to 4^+]$	50.0^{+47}_{-40}	205.5^{+196}_{-167}	168.24	248.98
$\mathrm{B}[E2; 4^+ \to 6^+]$	48.9^{+23}_{-13}	201.1^{+95}_{-53}	148.70	220.06
$\mathrm{B}[E2; 6^+ \to 8^+]$	n.a.	n.a.	140.92	208.55

4 Conclusion

The low-lying spectrum and the electromagnetic transitions of ^{24}Mg have been investigated in the framework of the geometric α-cluster model, presented in Ref. [43]. In the latter, an approximation scheme for the implementation of the coupling between rotational and vibrational motion, based on the Watson Hamiltonian [46], has been introduced [42].

The square bipyramid with $\mathcal{D}_{4h}$ symmetry [37, 38] has been reproposed as an equilibrium α-cluster configuration for ^{24}Mg. Due to the significant amount of spectroscopic data recorded since then, all the 9 predicted singly-excited rotational bands have been identified [42]. The normal-mode vibrations of the 6α-structure permitted to bring out the connection between certain normal modes (A_{1g}, A_{2u}, E_g) and low-energy cluster-decay channels. Essential support to the $\mathcal{D}_{4h}$-symmetric *ansatz* has been provided by the calculated M1 and E2 moments as well as the intraband and interband γ-transition strengths between the identified α-cluster states of ^{24}Mg, detailed in Ref. [42].

The perturbative application of the GαCM at NLO [42] is envisaged, since the rotation-vibration coupling is responsible of the observed changes in the nuclear moments of inertia in the excited rotational bands. Additionally, the tentative inspection of doubly-excited bands, with special attention to neighbour states of decay thresholds at 13.93 MeV (^{12}C + ^{12}C), 14.05 MeV (2α + ^{16}O) and 21.21 MeV (3α + ^{12}C) is planned.

The development of new facilities such as the *variable energy gamma system* (VEGA) at ELI-NP (Măgurele, Romania), wherein photo-excitation experiments in the energy range 1-20 MeV play a major role, is expected to enlarge the set of measured intraband and interband transition probabilities of ^{24}Mg, thus providing crucial tests for the validity of the present model.

Acknowledgements

This proceeding is part of a greater work started under the impulse of the co-author, who carried out the calculations in the initial phase. K.-H. S. was deeply interested in α-clustering in nuclei and contributed to a number of experimental investigations on EM properties of light nuclei [61]. G.S. acknowledges funding form the ESNT (CEA/DSM-DAM) and by the CNRS (UMR9012) and expresses gratitude to Serdar Elhatisari (King-Fahd University, Dhahran), Timo A. Lähde (FZ Jülich), Dean Lee (Michigan State University), Shihang Shen (Beihang University) and Vittorio Somà (CEA Paris-Saclay) for the discussions.

References

[1] K. Kato, H. Bando, *Prog. of Theor. Phys.* **62** (1979) 644-661.
[2] J. Cseh, G. Levai, W. Scheid, *Phys. Rev. C* **48** (1993) 1724.
[3] J. Cseh, J. Riczu, D.G. Jenkins, ArXiv:2312.08318 (2023).

[4] B. Buck, P.D.B. Hopkins, A.C. Merchant, *Nucl. Phys. A* **513** (1990) 75-114.

[5] M. Kimura, N. Furutachi, Y. Taniguchi, Y. Kanada-En'yo, H. Horiuchi, *Prog. Theor. Phys. Suppl.* **196** (2012) 176-183.

[6] M. Kimura, Y. Chiba, *J. Phys.: Conf. Ser.* **569** (2014) 012005.

[7] Y. Chiba, M. Kimura, *Phys. Rev. C* **91** (2015) 061302.

[8] M. Kimura, R. Yoshida, M. Isaka, *Prog. Theor. Phys.* **127** (2012) 287.

[9] Y. Chiba, M. Kimura, *Phys. Rev. C* **101** (2020) 024317.

[10] Y. Kanada-En'yo, K. Ogata, *Phys. Rev. C* **103** (2021) 024603.

[11] S. Elhatisari, L. Bovermann, Y.-Z. Ma, E. Epelbaum, D. Frame, F. Hildenbrand, Fabian, M. Kim, Y. Kim, H. Krebs, T.A. Lähde, D. Lee, N. Li, B.-N. Lu, U.-G. Meißner, G. Rupak, S. Shen, Y.-H. Song, G. Stellin, *Nature* **630** (2024) 59-63.

[12] S. Shen, S. Elhatisari, T.A. Lähde, D. Lee, B.-N. Lu, U-.G. Meißner, *Nature Comm.* **14** (2023) 2777.

[13] G. Stellin, S. Shen, T. Lähde, S. Elhatisari, "*Emergent geometry and duality in the ^{24}Mg nucleus*" (in preparation).

[14] A. Porro, T. Duguet, J.-P. Ebran, M. Frosini, R. Roth, V. Somà, ArXiv:2407.01325 (2024).

[15] W. Wefelmeier, *Zeitschr. für Physik* **107** (1937) 332.

[16] J.A. Wheeler, *Phys. Rev.* **52** (1937) 1083.

[17] L.R. Hafstad, E. Teller, *Phys. Rev.* **54** (1938) 681.

[18] G. Stellin, L. Fortunato, A. Vitturi, *J. of Phys. G* **43** (2016) 085104.

[19] A.E. Glassgold, A. Galonsky, *Phys. Rev.* **103** (1956) 701.

[20] R. Bijker, F. Iachello, *Ann. of Phys.* **298** (2002) 334.

[21] D. Jenkins, *J. of Phys. G* **43** (2016) 024003.

[22] O. Portilho, S.A. Coon, *Zeitsch. für Physik A* **290** (1979) 93-105.

[23] D.M. Dennison, *Phys. Rev.* **57** (1940) 454.

[24] R. Bijker, F. Iachello, *Nucl. Phys. A* **957** (2017) 154-176.

[25] L. Fortunato, *Eur. Phys. J. Web of Conf.* **311** (2024) 00015.

[26] Y. Ronen, N. Barnea, W. Leidemann, *Few-Body Syst.* **38** (2006) 97-101.

[27] R. Bijker, F. Iachello, *Phys. Rev. Lett.* **112** (2014) 152501.

[28] R. Bijker, F. Iachello, *Nucl. Phys. A* **1006** (2021) 122077.

[29] J. Dudek, D. Curien, I. Dedes, K. Mazurek, S. Tagami, Y.R. Shimizu, T. Bhattacharjee, *Phys. Rev. C* **97** (2018) 021302.

[30] I. Dedes, J. Dudek, "$\mathcal{C}_{2v}$ *(Water Molecule) Symmetry Identified in an Actinide Nucleus* ^{236}U", SSNET 2024 Conference, Orsay, France (public communication).

[31] R. Bjiker, F. Iachello, *Phys. Rev. C* **61** (2000) 067305.

[32] R. Bijker, F. Iachello, *Prog. in Part. and Nucl. Phys.* **110** (2020) 103735.

[33] C.J. Halcrow, "*Skyrmions - beyond rigid body quantisation*", Ph.D. dissertation, Dept. of app. math. and theor. physics, University of Cambridge (2017).

[34] C.J. Halcrow, J.I. Rawlinson, *Phys. Rev. C* **102** (2020) 014314.

[35] J.I. Rawlinson, *Nucl. Phys. A* **975** (2018) 122-135.

[36] D.L. Nordström, J.A. Tunheim, G.H. Duffey, *Phys. Rev.* **145** (1966) 727.

[37] M. Bouten, *Nuovo Cimento* **26** (1962) 3895-3904.

[38] P.S. Hauge, G.H. Duffey, *Phys. Rev.* **152** (1966) 1023.

[39] D.M. Brink, H. Friedrich, A. Weiguny, C.W. Wong, *Phys. Lett. B* **33** (1970) 143.

[40] D.M. Brink, "*The Alpha-particle Model of light Nuclei*" in C. Bloch, *Proc. Int. School Phys. "Enrico Fermi"*, *Course* **XXXVI**, SIF Bologna and IOS Press Amsterdam (1965).

[41] W. Bauhoff, H. Schultheis, R. Schultheis, *Phys. Lett. B* **95** (1980) 5-8.

[42] G. Stellin, "*Spectrum and electromagnetic properties of* ^{24}Mg *in a macroscopic* α*-cluster model: evidence of* $\mathcal{D}_{4h}$ *symmetry*" (in preparation).

[43] G. Stellin, K.-H. Speidel, "*Electromagnetic selection rules for* ^{24}Mg *in a* 6α *cluster model with* $\mathcal{D}_{4h}$ *symmetry*" (submitted to the *J. Phys. G.*), ArXiv:2412.17782 (2024).

[44] G. Stellin, K.-H. Speidel, "*Spectrum and electromagnetic properties of* ^{24}*Mg in the Geometric* α*-cluster Model with* $\mathcal{D}_{4h}$ *symmetry at leading order*" (extended version), ArXiv:2510.24522 (2025).

[45] G. Stellin, "*Simmetrie e rotovibrazioni di nuclei* α*-coniugati*", M.Sc. dissertation, Dipartimento di fisica e astronomia, Universit degli Studi di Padova (2015).

[46] J.K.G. Watson, *Mol. Phys.* **15** (1968) 479-490.

[47] R.L. Carter, *Molecular Symmetry and Group Theory* (John Wiley & Sons, 1997).

[48] P.R. Bunker, P.R. Jensen, *Fundamentals of Molecular Symmetry*, Institute of Physics, Series in Chem. Physics (CRC Press, 2004).

[49] M. Piccardo, J. Bloino, V. Barone, *Int. J. Quantum Chem.* **115** (2015) 948-982.

[50] J. Van de Wiele, *Annales de Physique* **26** (2001) 1-169.

[51] A. Bohr, B. Mottelson, *Nuclear Structure* **2**, "Nuclear deformations" (W.A. Benjamin, Inc., Advanced Book Program, Reading, 1975).

[52] P.S. Hauge, S.A. Williams, G.H. Duffey, *Phys. Rev. C* **4** (1971) 1044.

[53] L. Fortunato, G. Stellin, A. Vitturi, *Few Body Syst.* **58** (2017) 19.

[54] Y. Fujikawa, T. Kawabata, S. Adachi, S. Enyo, T. Furuno, Y. Hijikata, K. Himi, K. Hirose, Y. Honda, K. Inaba, H. Makii, K. Miyamoto, M. Murata, K. Nishio, S. Okamoto, R. Orlandi, K. Sakanashi, F. Suzaki, S. Tsuji, K. Yahiro, J. Zenihiro, *Phys. Lett. B* **848** (2024) 138384.

[55] J.D. Garrett, H.T. Fortune, R. Middleton, W. Scholz, *Phys. Rev. C* **18** (1978) 2032.

[56] L.K. Fifield, E.F. Garman, M.J. Hurts, T.J.M. Symons, F. Watt, C.H. Zimmerman, K.W. Allen, *Nucl. Phys. A* **322** (1979) 1-12.

[57] M.S. Basunia, A. Chakraborty, *Nucl. Data Sheets* **186** (2022)3-262.

[58] I. Angeli, K.P. Marinova, *Atom. Data Nucl. Data Tab.* **99** (2013) 69-95.

[59] A. Kusoglu, A.E. Stuchbery, G. Georgiev, B.A. Brown, A. Goasduff, L. Atanasova, D.L. Balabanski, M. Bostan, M. Danchev, P. Detistov, K.A. Gladnishki, J. Ljungvall, I. Matea, D. Radeck, C. Sotty, I. Stefan, D. Verney, D.T. Yordanov, *Phys. Rev. Lett.* **114** (2015) 062501.

[60] R.B. Firestone, *Nucl. Data Sheets* **108** (2007) 2319-2392.

[61] G. Stellin, K.-H. Speidel, U.-G. Meißner, *Eur. Phys. J. A* **58** (2022) 208.

[62] J.R. Marinelli, J.R. Moreira, *Phys. Rev. C* **39** (1989) 1242-1246.

[63] H.K. Issa, G.N. Flaiyh, *Iraqi J. Phys.* **23** (2025) 20-30.